Journal of ELECTRONIC MATERIALS, Vol. 38, No. 10, 2009
DOI: 10.1007/s11664-009-0874-4

Regular Issue Paper

Thermodynamic Assessment of the Au-Co-Sn Ternary System

H.Q. DONG,[1] S. JIN,[1] L.G. ZHANG,[1] J.S. WANG,[1] X.M. TAO,[1] H.S. LIU,[1,2,3] and Z.P. JIN[1,2]

1.—School of Materials Science and Engineering, Central South University, Changsha, Hunan Province 410083, P.R. China. 2.—The Key Lab of Non-Ferrous Metal Materials Science and Engineering, Educational Ministry, Changsha, P.R. China. 3.—e-mail: hsliu@mail.csu.edu.cn

Phase relationships in the Au-Co-Sn ternary system have been thermodynamically assessed by using the CALPHAD technique. The existing thermodynamic descriptions of the binary Au-Sn and Co-Sn systems were improved by incorporating the *ab initio* calculated enthalpies of formation of the intermetallic compounds including AuSn, CoSn, $AuSn_2$, and $AuSn_4$. For consistency, the Au-Co system was reassessed on the basis of the same pure element data as adopted for the Au-Sn and Co-Sn systems. With the combination of the three binary descriptions, the Au-Co-Sn ternary system was assessed by taking into account the ternary solubility in the binary compounds and the formation of a ternary compound. The obtained set of thermodynamic parameters can reproduce the measured phase equilibria at 380°C. The isothermal section at 396°C, the CoSn-Au and Au-SnCo vertical sections, and the liquidus projection were also calculated.

Key words: Au-Co-Sn, CALPHAD, thermodynamic assessment, *ab initio* calculations

INTRODUCTION

In modern electronic packaging technology, solders serve the purpose of electrical conduction, mechanical support, and heat dissipation.[1,2] The reliability of solder joints is greatly affected by the forming of intermetallic compounds (IMC) during soldering and subsequent service.[3–5] So knowledge about the thermodynamics and kinetics of the interfacial reaction between solder and the metal pad (or under bump metallization, UBM) is important for electronic packaging.[3]

As one of the mature soldering alloys, Au-Sn (20 wt.% Sn) has historically been employed in the microelectronics industry for fluxless hermetic lid sealing and die attachment applications.[6–10] Recently, Co has been considered as a candidate UBM material[11,12] and candidate alloying element in Pb-free solders.[13,14] Additionally, there is a little research about the phase diagram of the Sn-Co solder and the interfacial reaction between lead-free solder and Au as the UBM material.[14–17] In order to accelerate the development of new soldering alloys and predict the interfacial reactions in the Au-Sn/Co and Sn-Co/Au systems more efficiently, thermodynamic information for the related system, i.e., Au-Co-Sn, is essential.

So far, only one isothermal section of the Au-Co-Sn ternary system at 380°C (653 K) has been experimentally determined.[18] In order to establish a thermodynamic database for this system, a precise thermodynamic description was performed in this study by using the calculation of phase diagram (CALPHAD) technique.[19] First, the necessary thermodynamic properties of some phases were calculated by *ab initio* calculations.[20,21] Then, the thermodynamic parameters of the Au-Co binary system were reassessed and those of the Au-Sn and Co-Sn binary systems slightly modified from the reported versions.[22,23] Finally, the Au-Co-Sn system was extrapolated by using Thermo-calc software[24] along with Pandat.[25]

(Received September 17, 2008; accepted June 10, 2009; published online July 1, 2009)

EVALUATION OF THE AVAILABLE INFORMATION

The Au-Sn and Co-Sn Binary Systems

The phase diagram of the Au-Sn system has already been thermodynamically optimized,[23,26] and good agreement was achieved between experimental data and calculated values. In particular, the dependence of the enthalpy of mixing of the liquid Au-Sn alloys on temperature has been taken into account.[23] However, no information was provided on the enthalpy of formation of the IMCs except for AuSn when this system was optimized.[23] In order to obtain a more reliable description of the Au-Sn binary system, *ab initio* calculation was employed to find the enthalpies of formation of $AuSn_2$ and $AuSn_4$ in this work.

In addition, as shown in the section "The Au-Co-Sn Ternary System," the ternary solubility of Co in AuSn (NiAs-type structure) reaches 12 at.%. This suggests that the enthalpy of formation of the CoSn metastable phase with the NiAs structure will be essential when phase relations in the Au-Co-Sn ternary system are extrapolated. Hence, the enthalpy of formation of the assumed compound CoSn with the NiAs structure is also calculated by an *ab initio* approach.

Phase equilibria in the Co-Sn binary system have also been optimized.[14,22] Compared with Ref. 14, Ref. 22 took more experiments into consideration, such as information about $CoSn_3$ and the homogeneity range of βCo_3Sn_2. Thus, the thermodynamic parameters of most phases are adopted from Ref. 22 except for the parameters of the $CoSn_2$ and $CoSn_3$ phases, which will be modified to reproduce the ternary phase relations.

The Au-Co Binary System

Okamoto et al.[27] and Korb[28] assessed the phase diagram of the Au-Co binary system. However, when Okamoto et al.[27] finished the optimization of the Au-Co system, the new lattice stabilities collected by Dinsdale[29] had not been published. In addition, Korb[28] had not published his work on this system. In order to set up a consistent database of the Au-Co-related multicomponent system, thermodynamic reassessment of the Au-Co system was required

The phase boundaries of the Au-Co system were well determined.[30–36] In this system, an eutectic and an eutectoid were detected, as listed in Table I. Berezutsky et al.[37] studied activities of Au in liquid Au-Co alloys using vapor pressure techniques. Activities of Co in Au-Co alloys were extensively measured.[35,37–39] First, by using electromotive force measurements, Kubil and Alcol[38] measured the activity of Co in Au-rich solid solutions at 1150 K. Subsequently, the activity of Co in the liquid Au-Co alloy was determined from the equilibrium with CoO by using a CO/CO_2 gas mixture of known partial pressure.[39] Later, by measuring the vapor pressure, activities of Co in liquid alloy at 1623 K were studied.[37] Then activities of Co in the liquid alloys at 1573 K and in Au-rich solid solutions at 1150 K were measured by Taskinen.[35] These sets of activities of Co are compatible with each other except for those reported by Wang and Toguri,[39] which exhibited some negative deviation from the results of Taskinen[35] and Berezutskiy et al.[37] Considering the lower reliability of the method employed, the data of Wang and Toguri[39] were given less weight during optimization. The enthalpies of mixing of the solid solutions were determined by calorimetry for alloys with high Au concentration[35,40,41] with little dispersion existing in these data.

The Au-Co-Sn Ternary System

Only the isothermal section at 380°C (653 K) for the Au-Co-Sn system was experimentally constructed by powder x-ray diffraction, metallography, electron microprobe analysis, and thermal analysis.[18] A ternary compound phase (denoted $\tau 1$) was detected; it melted peritectically at 395°C (668 K):

$$\tau 1 \rightarrow L + CoSn + Au_{15}Co_{41}Sn_{44},$$

where $Au_{15}Co_{41}Sn_{44}$ belongs to the βCo_3Sn_2 phase with ternary solubility of Au.

According to Ref. 18, Au(fcc) dissolved < 1 at.% Co and 7 at.% Sn, while Co(hcp) dissolved < 1 at.% of both Au and Sn. At 653 K, the solubility of the third element in the binary intermetallic phases, ζ(hcp), $\beta(Au_{10}Sn)$, CoSn, and $CoSn_2$, was extremely limited, whereas both AuSn and αCo_3Sn_2 had an extended range of ternary homogeneity, up to 12 at.% Co and 23 at.% Au, respectively. Hence, the ternary solubilities in AuSn and αCo_3Sn_2 should be taken into account when the related phase relations are assessed.

Table I. Invariant Reactions in the Au-Co Binary System

Reaction	Composition (at.% Co)			*T* (K)	Type	Reference
$L \Leftrightarrow Au + \alpha Co$	24.8	23	98.1	1269.5	Eutectic	Okamoto et al.[27]
	26.2	20.8	97.7	1270.4	Eutectic	This work
$\alpha Co \Leftrightarrow Au + \varepsilon Co$	99.95	0.2	–	695	Eutectoid	Okamoto et al.[27]
	99.9	0.9	99.93	694	Eutectoid	This work

CALCULATION METHOD

Ab Initio Calculations

In order to obtain the enthalpy of formation of some compounds (i.e., the hypothesized compound CoSn with the NiAs-type structure, AuSn, $AuSn_2$, and $AuSn_4$), an *ab initio* approach was performed by using the scalar relativistic all-electron Blöchl's projector augmented-wave method[42,43] within the generalized gradient approximation (GGA), as implemented in the highly efficient Vienna *ab initio* simulation package (VASP).[20,21] For the GGA exchange-correlation function, the Perdew–Wang parameterization (PW91)[44,45] was employed. A constant plane–wave energy cutoff of 450 eV was used for A_xB_y compounds. Brillouin-zone integrations were performed using Monkhorst–Pack[46] k-point meshes, and the Methfessel–Paxton[47] technique with smearing parameter of 0.2 eV. The reciprocal space (k-point) meshes were increased to achieve convergence to a precision of 5 meV/atom. The total energy converged numerically to less than 1×10^{-6} eV/unit with respect to electronic, ionic, and unit cell degrees of freedom, and the latter two were relaxed using Hellman–Feynman forces with a preconditioned conjugated gradient algorithm. After structural optimization, the Hellman–Feynman forces on each ion were less than 0.01 eV/Å. All calculations were performed using the "high" setting within VASP to avoid wrap-around errors. In addition, spin polarization was used in all calculations.

The enthalpies of formation of the IMCs were calculated by the following equation:

$$\Delta H(A_xB_y) = E_{\text{total}}(A_xB_y) - xE_{\text{total}}(A) - yE_{\text{total}}(B), \tag{1}$$

where $E_{\text{total}}(A_xB_y)$, $E_{\text{total}}(A)$, and $E_{\text{total}}(B)$ are the calculated total energies (per atom at T = 0 K) of the IMCs for pure A and B, respectively.

Thermodynamic Models

For lattice stabilities of the elements Au, Co, and Sn refer to Dinsdale.[29] Different models were employed to describe the solution phases and IMCs of the Au-Co-Sn system.

Solution Phases: Liquid, Au(fcc), Co(fcc), Co(hcp), and Sn(bct)

An ordinary substitutional solution model was applied to depict the liquid, fcc, hcp, and bct terminal solutions. The molar Gibbs energy of a solution phase Φ (Φ = liquid, fcc, hcp, bct) can be represented as a sum of the Gibbs energy for the pure components, the ideal entropy term describing a random mixing of the components, and the excess Gibbs energy describing the deviation from ideal mixing, i.e.,

$$G^{\phi} = \sum_{i=\text{Au,Co,Sn}} x_i {}^0G_i^{\phi} + RT \sum_{i=\text{Au,Co,Sn}} x_i \ln(x_i) + {}^{\text{ex}}G^{\phi}, \tag{2}$$

where R is the gas constant, T is the temperature in Kelvin, x_i is the molar fraction of component i (i = Au, Co, and Sn), and ${}^0G_i^{\phi}$ is the molar Gibbs energy of the pure element i in the ϕ state. The excess term is formulated as

$$\begin{aligned} {}^{\text{ex}}G^{\phi} = {} & x_{\text{Au}}x_{\text{Co}} \sum_{j=0,1\ldots}^{N} {}^{(j)}L_{\text{Au,Co}}^{\phi}(x_{\text{Au}} - x_{\text{Co}})^j \\ & + x_{\text{Au}}x_{\text{Sn}} \sum_{j=0,1\ldots}^{N} {}^{(j)}L_{\text{Au,Sn}}^{\phi}(x_{\text{Au}} - x_{\text{Sn}})^j \\ & + x_{\text{Co}}x_{\text{Sn}} \sum_{j=0,1\ldots}^{N} {}^{(j)}L_{\text{Co,Sn}}^{\phi}(x_{\text{Co}} - x_{\text{Sn}})^j \\ & + x_{\text{Au}}x_{\text{Co}}x_{\text{Sn}}L_{\text{Au,Co,Sn}}^{\phi}, \end{aligned} \tag{3}$$

where ${}^{(j)}L_{\text{Au,Sn}}^{\phi}$ and ${}^{(j)}L_{\text{Co,Sn}}^{\phi}$ are taken directly from Liu et al.[23] and Jiang et al.,[22] respectively. The parameter ${}^{(j)}L_{\text{Au,Co}}$ is expressed as

$${}^{(j)}L_{\text{Au,Co}}^{\phi} = E_j + F_jT \tag{4}$$

with parameters E_j and F_j to be optimized. Due to the lack of experimental data, the ternary interaction parameters $L_{\text{Au,Co,Sn}}^{\phi}$ will not be optimized and are set to zero.

Binary Intermetallic Phases

To fit the ternary phase equilibria, thermodynamic parameters of $CoSn_2$ and $CoSn_3$ obtained by Jiang et al.[22] should be modified slightly, i.e.,

$$G_{\text{Co:Sn}}^{\text{CoSn}_2} = 03333\,{}^0G_{\text{Co}}^{\text{hcp}} + 0.6667\,{}^0G_{\text{Sn}}^{\text{bct}} + C + DT \tag{5}$$

$$G_{\text{Co:Sn}}^{\text{CoSn}_3} = 0.25\,{}^0G_{\text{Co}}^{\text{hcp}} + 0.75\,{}^0G_{\text{Sn}}^{\text{bct}} + C_1 + D_1T \tag{6}$$

with C, D, C_1, and D_1 to be reassessed in the present work.

The Co_3Sn_2 phase has an order–disorder transformation from βCo_3Sn_2 to αCo_3Sn_2, and βCo_3Sn_2 and AuSn belong to the $B8_1$-type NiAs structure.[48] According to the work of Jiang et al.,[22] the same model was adopted to treat βCo_3Sn_2 and αCo_3Sn_2, which can reduce the number of parameters to be optimized. However, such a treatment will lead to difficulties when the ternary or quaternary solubility is considered. For simplicity, different models are employed to describe AuSn and βCo_3Sn_2 or αCo_3Sn_2.

The extension of the homogeneity range of Sn is virtually unaffected by Co content in AuSn. So a two-sublattice model (Au,Co):(Sn) is adopted.

Hence, the Gibbs energy of the NiAs-type AuSn is formulated as

$$G^{\mathrm{AuSn}} = Y^{\mathrm{I}}_{\mathrm{Au}} G_{\mathrm{Au:Sn}} + Y^{\mathrm{I}}_{\mathrm{Co}} G_{\mathrm{Co:Sn}} + 0.5RT(Y^{\mathrm{I}}_{\mathrm{Au}} \ln Y^{\mathrm{I}}_{\mathrm{Au}} + Y^{\mathrm{I}}_{\mathrm{Co}} \ln Y^{\mathrm{I}}_{\mathrm{Co}}) + Y^{\mathrm{I}}_{\mathrm{Au}} Y^{\mathrm{I}}_{\mathrm{Co}} \left(\sum_{j=0,1\ldots} {}^{j}L_{\mathrm{Au,Co:Sn}} (Y_{\mathrm{Au}} - Y_{\mathrm{Co}})^{j} \right), \quad (7)$$

where $G_{\mathrm{Au:Sn}}$ is taken from Ref. 23, and the Gibbs energy of the assumed CoSn compound of AuSn structure, $G_{\mathrm{Au:Sn}}$, is expressed as

$$G_{\mathrm{Co:Sn}} = 0.5{}^{0}G^{\mathrm{hcp}}_{\mathrm{Co}} + 0.5{}^{0}G^{\mathrm{bct}}_{\mathrm{Sn}} + C_2 + D_2 T. \quad (8)$$

Here C_2 and D_2 are the adjusted parameters to be optimized, and C_2 is assessed on the basis of an *ab initio* calculation.

According to Ref. 18 the αCo_3Sn_2 phase also shows an extended ternary range of homogeneity (up to 23 at.% Au) at 653 K, which almost parallels the Au-Co boundary. This implies that the Co site in the lattice can be partly taken up by Au atoms. According to the work of Jiang et al.,[22] a four-sublattice model $(Au,Co)_1:(Sn)_1:(Co,V_a)_{0.5}:(Co,V_a)_{0.5}$, with V_a denoting vacancy, is introduced, and the Gibbs energy is expressed as

$$\begin{aligned} G^{\mathrm{Co_3Sn_2}} = & \sum_i \sum_j \sum_k Y^{\mathrm{I}}_i Y^{\mathrm{III}}_j Y^{\mathrm{IV}}_k G_{i:\mathrm{Sn};j:k} \\ & + RT(Y^{\mathrm{I}}_{\mathrm{Au}} \ln Y^{\mathrm{I}}_{\mathrm{Au}} + Y^{\mathrm{I}}_{\mathrm{Co}} \ln Y^{\mathrm{I}}_{\mathrm{Co}}) \\ & + 0.5RT(Y^{\mathrm{III}}_{\mathrm{Co}} \ln Y^{\mathrm{III}}_{\mathrm{Co}} + Y^{\mathrm{III}}_{\mathrm{V_a}} \ln Y^{\mathrm{III}}_{\mathrm{V_a}}) \\ & + 0.5RT(Y^{\mathrm{IV}}_{\mathrm{Co}} \ln Y^{\mathrm{IV}}_{\mathrm{Co}} + Y^{\mathrm{IV}}_{\mathrm{V_a}} \ln Y^{\mathrm{IV}}_{\mathrm{V_a}}) \\ & + \sum_l \sum_{i>l} \sum_j \sum_k Y^{\mathrm{I}}_l Y^{\mathrm{I}}_i Y^{\mathrm{III}}_j Y^{\mathrm{IV}}_k L_{l,i:\mathrm{Sn};j:k} \\ & + \sum_l \sum_j \sum_{k>j} \sum_n Y^{\mathrm{I}}_l Y^{\mathrm{III}}_j Y^{\mathrm{III}}_k Y^{\mathrm{IV}}_n L_{l:\mathrm{Sn};j,k:n} \\ & + \sum_l \sum_j \sum_k \sum_{n>k} Y^{\mathrm{I}}_l Y^{\mathrm{III}}_j Y^{\mathrm{IV}}_k Y^{\mathrm{IV}}_n L_{l:\mathrm{Sn};j;k,n} \quad (9) \end{aligned}$$

where l, i denote Au and Co, and j, k, n indicate Co and V_a, while $G_{\mathrm{Co:Sn:Co:Co}}$, $G_{\mathrm{Co:Sn:V_a:Co}}$, $G_{\mathrm{Co:Sn:Co:V_a}}$, and $G_{\mathrm{Co:Sn:V_a:V_a}}$ are taken directly from Jiang et al.[22] Other parameters are to be optimized in this work.

Ternary IMCs

$\tau 1$ is reported to have the stoichiometry $Au_{0.15}Co_{0.25}Sn_{0.6}$, of which the Gibbs energy is modeled with the following expression:

$$G_{\tau 1} = 0.15{}^{0}G^{\mathrm{fcc}}_{\mathrm{Au}} + 0.25{}^{0}G^{\mathrm{hcp}}_{\mathrm{Co}} + 0.6{}^{0}G^{\mathrm{bct}}_{\mathrm{Sn}} + C_3 + D_3 T \quad (10)$$

with parameters C_3 and D_3 to be optimized.

RESULTS AND DISCUSSION

Ab Initio Calculations

To assess the phase relationships in the binary system better and extrapolate to the ternary system, the enthalpy of formation of the NiAs-type AuSn, hypothesized NiAs-type CoSn, $AuSn_2$, and $AuSn_4$ were calculated by an *ab initio* method. The corresponding results are listed in Table II. The calculated enthalpy of formation of AuSn is −18.77 kJ/g·atom, which seems to deviate greatly from the reported experimental value,[49] i.e., −14.88 kJ/g·atom. In that case diamond-Sn was the reference state for the determined enthalpy of formation,[49] while bct-Sn was adopted by the *ab initio* calculation in this work. In order to compare the two values, the same reference state of Sn should be employed. So the experimental data of AuSn at 78 K is modified to be −15.69 kJ/g·atom with the reference state of Sn(bct). The *ab initio* calculation value, −18.77 kJ/g·atom, is still slightly more positive than the modified experimental data.

Generally, temperature dissimilarity (78 K for measurement and 0 K for the *ab initio* approaches) may lead to some deviation between the experimental

Table II. Enthalpies of Formation at 0 K Obtained by *Ab Initio* Calculation and Assessed in This Work at 10 K. Reference states: Au(fcc), Sn(bct), and Co(hcp)

Phase	Experimental (kJ/mol) at 78 K	*Ab Initio*, This Work (kJ/mol)	Assessed This Work (kJ/mol)	Pearson Symbol[50]	Lattice Parameter (Å)
NiAs-type					
CoSn	–	−3.82	−3.75	–	a = 3.362 b = 1.940 c = 5.258
AuSn	−15.69 modified −14.88 (Ref. 49)	−18.77	−15.75	hP4	a = 3.824 b = 2.208 c = 5.677
$AuSn_2$	–	−13.10	−13.38	oP24	a = 7.025 b = 7.182 c = 12.12
$PdSn_4$ type, $AuSn_4$	–	−7.19	−7.20	oC20	a = 6.051 b = 3.032 c = 5.980

Table III. Thermodynamic Parameters of the Au-Co-Sn Ternary System Obtained in This Study

Phase	Thermodynamic Parameters	Reference
Liquid model: (Au,Co,Sn)	${}^{0}L^{\mathrm{Liq}}_{\mathrm{Au,Co}} = 18493.31 - 2.00847T$	This work
	${}^{1}L^{\mathrm{Liq}}_{\mathrm{Au,Co}} = -825.79 - 3.33314T$	This work
	${}^{2}L^{\mathrm{Liq}}_{\mathrm{Au,Co}} = -2178.10$	This work
	${}^{0}L^{\mathrm{Liq}}_{\mathrm{Au,Sn}} = -48822.94 + 19.6767T - 2.8429T * \ln(T)$	Liu et al.[23]
	${}^{1}L^{\mathrm{Liq}}_{\mathrm{Au,Sn}} = -17990.36 + 0.7892T$	Liu et al.[23]
	${}^{2}L^{\mathrm{Liq}}_{\mathrm{Au,Sn}} = -5222.53$	Liu et al.[23]
	${}^{0}L^{\mathrm{Liq}}_{\mathrm{Co,Sn}} = -111091.08 + 577.90398T - 66.556343T * \ln(T)$	Jiang et al.[22]
	${}^{1}L^{\mathrm{Liq}}_{\mathrm{Co,Sn}} = -44585.348 + 222.13120T - 27.092377T * \ln(T)$	Jiang et al.[22]
	${}^{2}L^{\mathrm{Liq}}_{\mathrm{Co,Sn}} = 2252$	Jiang et al.[22]
$\tau 1$ model: $Au_{0.15}Co_{0.25}Sn_{0.6}$	$G^{\tau 1}_{\mathrm{Au,Co,Sn}} = -15900 + 2.2T + 0.15GHSERAU + 0.25GHSERCO + 0.6GHSERSN$	This work
Fcc model: (Au,Co,Sn)	${}^{0}L^{\mathrm{fcc}}_{\mathrm{Au,Co}} = 31876.94 - 4.16399T$	This work
	${}^{1}L^{\mathrm{fcc}}_{\mathrm{Au,Co}} = 2149.78 - 10.02798T$	This work
	${}^{2}L^{\mathrm{fcc}}_{\mathrm{Au,Co}} = -1117.93$	This work
	${}^{0}L^{\mathrm{fcc}}_{\mathrm{Co,Sn}} = -13699.002 + 15.964973T$	Jiang et al.[22]
	${}^{0}L^{\mathrm{Fcc}}_{\mathrm{Au,Sn}} = -28802.84 - 5.5753T$	Liu et al.[23]
	${}^{1}L^{\mathrm{fcc}}_{\mathrm{Au,Sn}} = 8515.07 - 11.7873T$	Liu et al.[23]
	${}^{2}L^{\mathrm{fcc}}_{\mathrm{Au,Sn}} = 368.57$	Liu et al.[23]
Co_3Sn_2 model: $(Au,Co)_1Sn_1(Co,Va)_{0.5}(Co,Sn)_{0.5}$	$G^{\mathrm{Co_3Sn_2}}_{\mathrm{Au:Sn:Co:Co}} = -28052.6 + GHSERCO + GHSERSN + GHSERAU$	This work
	$G^{\mathrm{Co_3Sn_2}}_{\mathrm{Au:Sn:V_a:V_a}} = -29000 + 15T + GHSERSN + GHSERAU$	This work
	$G^{\mathrm{Co_3Sn_2}}_{\mathrm{Au:Sn:Co:V_a}} = -43248.035 + 15.75233T + 0.5GHSERCO + GHSERSN + GHSERAU$	This work
	$G^{\mathrm{Co_3Sn_2}}_{\mathrm{Au:Sn:V_a:Co}} = -1000 + 0.5GHSERCO + GHSERSN + GHSERAU$	This work
	${}^{0}L^{\mathrm{Co_3Sn_2}}_{\mathrm{Au:Sn:Co:Co,V_a}} = -15000 + 10T$	This work
	${}^{0}L^{\mathrm{Co_3Sn_2}}_{\mathrm{Au:Sn:Co,V_a:Co}} = -20272$	This work
	$G^{\mathrm{Co_3Sn_2}}_{\mathrm{Co:Sn:Co:Co}} = -29681.113 + 2GHSERCO + GHSERSN$	Jiang et al.[22]
	$G^{\mathrm{Co_3Sn_2}}_{\mathrm{Co:Sn:V_a:V_a}} = -32053.837 + 13.504669T + GHSERCO + GHSERSN$	Jiang et al.[22]
	$G^{\mathrm{Co_3Sn_2}}_{\mathrm{Co:Sn:V_a:Co}} = -46488.035 + 15.7523345T + 1.5GHSERCO + GHSERSN$	Jiang et al.[22]
	$G^{\mathrm{Co_3Sn_2}}_{\mathrm{Co:Sn:Co:V_a}} = -46488.035 + 15.7523345T + 1.5GHSERCO + GHSERSN$	Jiang et al.[22]
	${}^{0}L^{\mathrm{Co_3Sn_2}}_{\mathrm{Co:Sn:Co,V_a:Co}} = 13272.615875 - 9T$	Jiang et al.[22]
	${}^{0}L^{\mathrm{Co_3Sn_2}}_{\mathrm{Co:Sn:Co:Co,V_a}} = 13272.615875 - 9T$	Jiang et al.[22]
	${}^{0}L^{\mathrm{Co_3Sn_2}}_{\mathrm{Co:Sn:V_a:Co,V_a}} = -513.735875 - 9T$	Jiang et al.[22]
	${}^{0}L^{\mathrm{Co_3Sn_2}}_{\mathrm{Co:Sn:Co,V_a:V_a}} = -513.735875 - 9T$	Jiang et al.[22]
	${}^{1}L^{\mathrm{Co_3Sn_2}}_{\mathrm{Co:Sn:Co,V_a:V_a}} = 1631.058625$	Jiang et al.[22]
	${}^{1}L^{\mathrm{Co_3Sn_2}}_{\mathrm{Co:Sn:Co,V_a:Co}} = 1631.058625$	Jiang et al.[22]
	${}^{1}L^{\mathrm{Co_3Sn_2}}_{\mathrm{Co:Sn:Co:Co,V_a}} = 1631.058625$	Jiang et al.[22]
	${}^{1}L^{\mathrm{Co_3Sn_2}}_{\mathrm{Co:Sn:V_a:Co,V_a}} = 1631.058625$	Jiang et al.[22]
$CoSn_2$ model: $Co_{0.333}Sn_{0.667}$	$G^{\mathrm{CoSn_2}}_{\mathrm{Co:Sn}} = -15700 + 4.09932T + 0.333GHSERCO + 0.667GHSERSN$	This work
$CoSn_3$ model: $Co_{0.25}Sn_{0.75}$	$G^{\mathrm{CoSn_3}}_{\mathrm{Co:Sn}} = -11475 + 1.930T + 0.25GHSERCO + 0.75GHSERSN$	This work
Hcp model: (Au,Co,Sn)	${}^{0}L^{\mathrm{hcp}}_{\mathrm{Au,Co}} = 30000$	This work
	${}^{0}L^{\mathrm{hcp}}_{\mathrm{Co,Sn}} = 7000$	Jiang et al.[22]
	${}^{0}L^{\mathrm{hcp}}_{\mathrm{Au,Sn}} = -13145.27 - 6.4932T$	Liu et al.[23]
	${}^{1}L^{\mathrm{hcp}}_{\mathrm{Au,Sn}} = -19184.81 - 25.1676T$	Liu et al.[23]
$AuSn_2$ model: $Au_{0.33333}Sn_{0.66667}$	$G^{\mathrm{AuSn_2}}_{\mathrm{Au:Sn}} = -13380 + 3.906T + 0.33333GHSERAU + 0.66667GHSERSN$	This work

Table III. Continued

Phase	Thermodynamic Parameters	Reference
$AuSn_4$ model: $Au_{0.2}Sn_{0.8}$	$G^{AuSn_4}_{Au:Sn} = -7201 - 0.22T + 0.2GHSERAU + 0.8GHSERSN$	This work
γ model: $Au_{0.84}Sn_{0.16}$	$G^{\gamma}_{Au:Sn} = -4065 - 3.3T + 0.84GHSERAU + 0.16GHSERSN$	This work
AuSn model: $(Au,Co)_1Sn_1$	$G^{AuSn}_{Au:Sn} = -31500 + 4.3039T + GHSERAU + GHSERSN$	This work
	$G^{AuSn}_{Co:Sn} = -7500 + GHSERCO + GHSERSN$	This work
	${}^0L^{AuSn}_{(Au,Co):Sn} = -28500 - 3.5T$	This work
β model: (Au,Sn)	${}^0L^{\beta}_{Au,Sn} = -13427.03 - 5.2576T$	Liu et al.[23]
	${}^1L^{\beta}_{Au,Sn} = -14823.13 - 21.1189T$	Liu et al.[23]
CoSn model: Co0.5Sn0.5	$G^{CoSn}_{Co:Sn} = -20900 + 5.8941642T + 0.5GHSERCO + GHSERSN$	Jiang et al.[22]

[1]GHSER means Gibbs energy relative to the standard element reference, i.e., the enthalpies of the pure elements in their defined reference phase at 298.15 K.

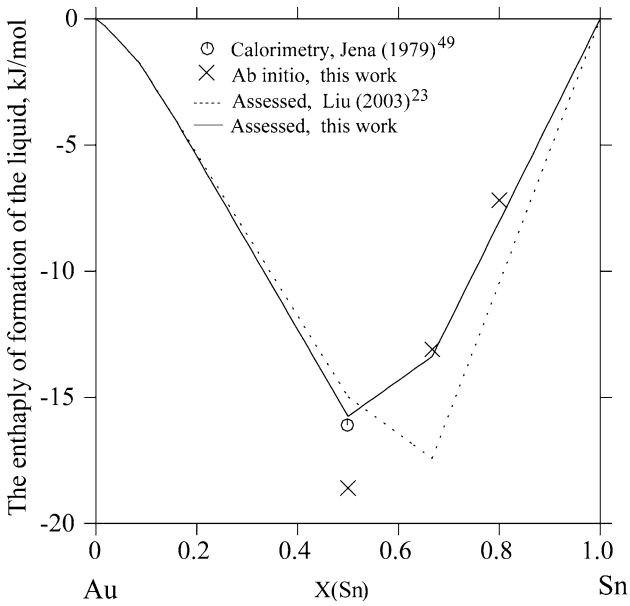

Fig. 1. Enthalpy of formation of the Au-Sn binary system at 298 K. Reference states: Au(fcc) and Sn(bct).

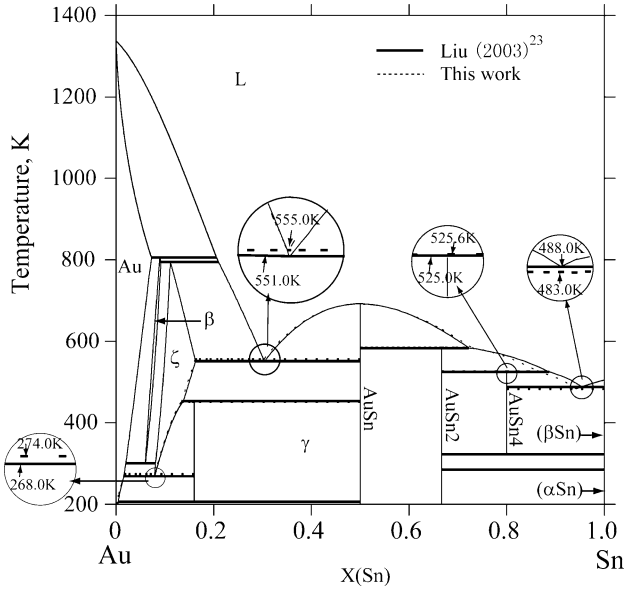

Fig. 2. Calculated phase diagram of the Au-Sn binary system.

data and the calculated value, but this kind of deviation is quite limited. The large difference may result from the treatment of the nonstoichiometry of AuSn in the *ab initio* calculation. According to previous research,[50] the NiAs-type AuSn compound has a narrow homogeneity range. Therefore, part of the Au and Sn sites in the lattice of the NiAs structure might be occupied by vacancies or mutually substituted to fit the alternative composition. Because the calculation capacity of our computer is limited, a simple cell was constructed with vacancy or mutual occupation not considered during the *ab initio* calculation. These may be the main reason leading to the deviation between the calculated enthalpy of formation of AuSn and the measured data.[49]

Meanwhile, during optimization, the enthalpies of formation obtained by the *ab initio* calculations (Table II) are only adopted as the initial data for some thermodynamic parameters of the assumed compound NiAs-type CoSn, $AuSn_2$, and $AuSn_4$. Compared with the weight given to the corresponding measured data, smaller weight is applied to these calculated values to fit the enthalpies of formation.

Thermodynamic Assessment

Table III lists the parameters evaluated by using the PARROT module in the Thermo-Calc software[24] based on the experimental and theoretical data for the phase diagram and thermodynamic properties. As discussed in the following sections, the present calculations reproduce most of the thermodynamic properties and phase boundary data.

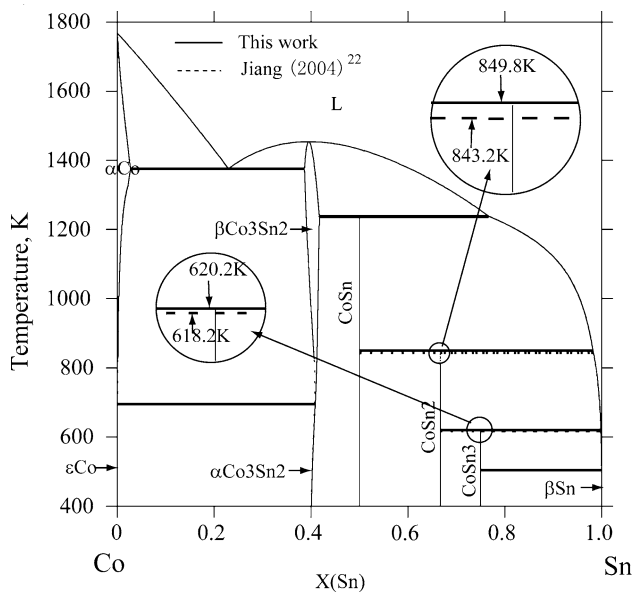

Fig. 3. Calculated phase diagram of the Co-Sn binary system.

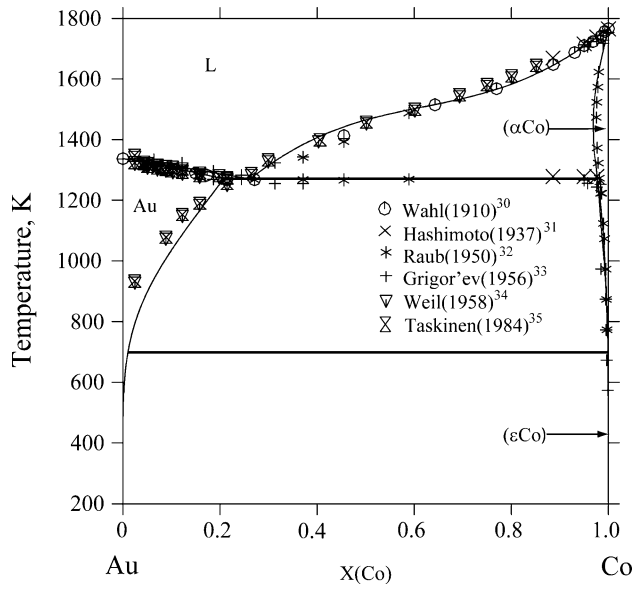

Fig. 4. Calculated phase boundary of the Au-Co binary system in comparison with the experimental data.

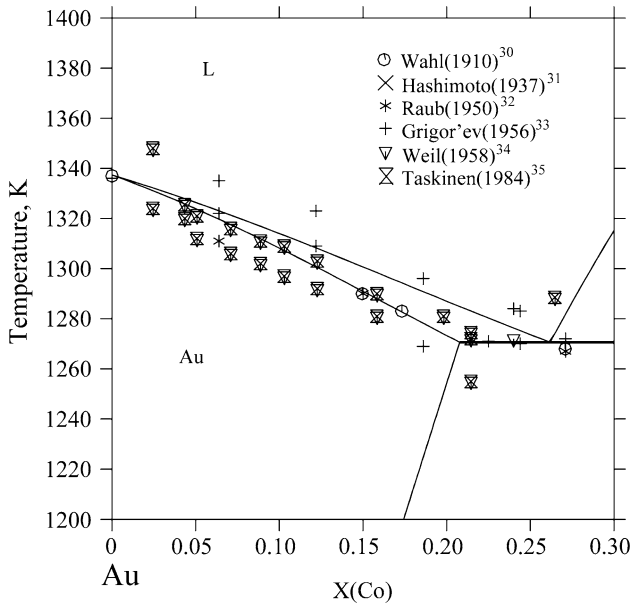

Fig. 5. Comparison between the calculated solidus and liquidus of the Au-rich part of the Au-Co system and measured phase boundaries.

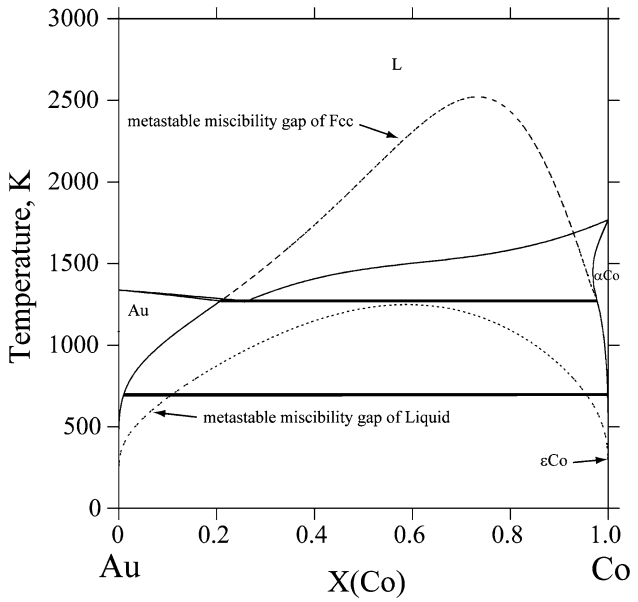

Fig. 6. Calculated phase diagram of the Au-Co binary system with metastable miscibility gaps of liquid and fcc.

The Au-Sn Binary System

Figure 1 shows the comparison of the enthalpy of formation calculated by CALPHAD with those by the *ab initio* approach. Along with the optimized phase equilibria (Fig. 2), it is obvious that the present assessment of the Au-Sn binary system is more reasonable.

The Co-Sn Binary System

In order to reproduce the ternary equilibria, thermodynamic parameters of $CoSn_2$ and $CoSn_3$ are changed slightly from the work of Jiang et al.[22] Figure 3 shows the comparison between the phase diagrams optimized in this work and that by Jiang et al.,[22] which illustrates that the two versions of the phase diagram are consistent.

The Au-Co Binary System

A comparison between the assessed phase diagram in this work and measured phase boundaries[30–36] is illustrated in Figs. 4 and 5. In addition

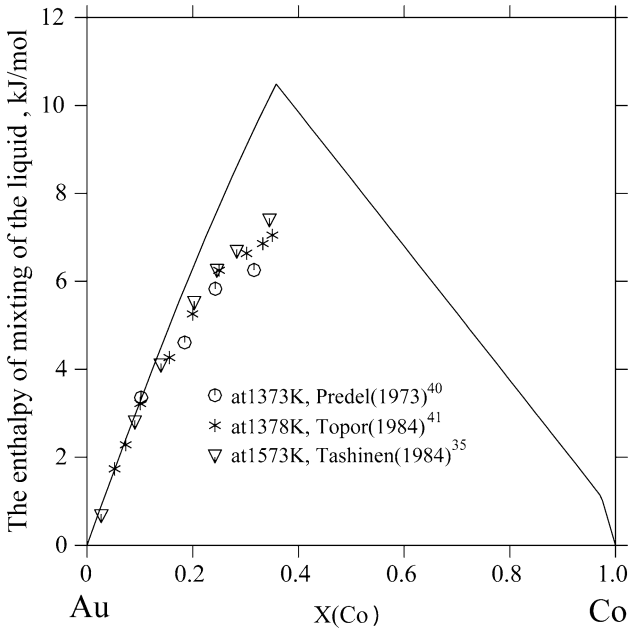

Fig. 7. Calculated enthalpies of mixing of the Au-Co alloys at 1378 K in comparison with experimental data. Reference states: Au(liquid) and Co(fcc).

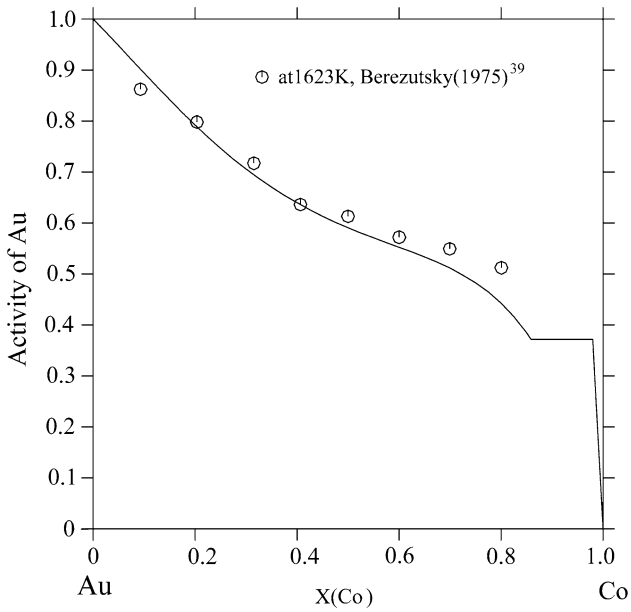

Fig. 8. Activities of Au in liquid Au-Co alloys at 1623 K with comparison between the calculated and measured data. Reference states: Au(liquid) and Co(liquid).

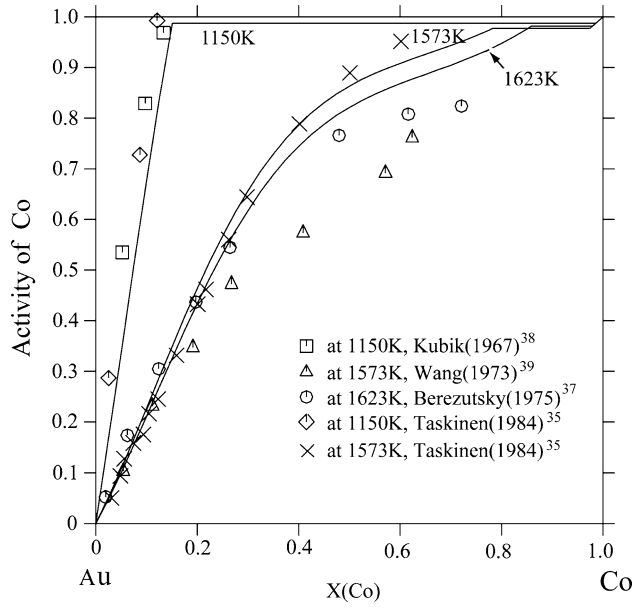

Fig. 9. Calculated activities of Co in liquid Au-Co alloys in comparison with the reported data. Reference states: Co(liquid) and Au(liquid) at 1573 K and 1623 K, Au(fcc) and Co(fcc) at 1150 K.

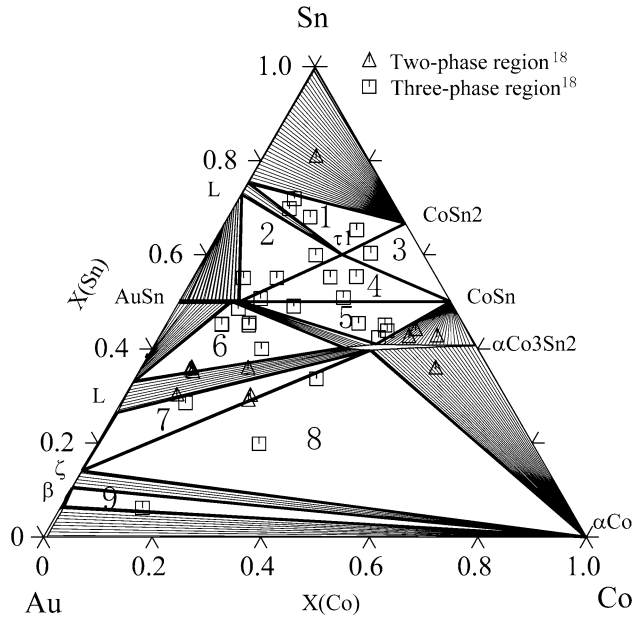

Fig. 10. Calculated isothermal section of the Au-Co-Sn system compared with measured phase equilibria[18] at 653 K.

the invariant reactions in the Au-Sn system are listed in Table I. As these reveal, good agreement was attained between the calculated phase relations and the corresponding measured relations. Metastable miscibility gaps of liquid and fcc are additionally calculated, as shown in Fig. 6. Both gaps are slightly asymmetric.

As illustrated in Fig. 7, the measured enthalpies of mixing of the liquid Au-Co alloys are reproduced by using the optimized parameters. Activities of Au (Fig. 8) and Co (Fig. 9) in the Au-Co alloys at various temperatures also fit well with the experimental data.

The Au-Co-Sn Ternary System

To date, there has been no thermochemical and liquidus projection information reported. Hence the

Table IV. Comparison of the Calculated Phase Equilibria with Experimental Results at 635 K

Region	Calculated Phases	Experimental Phases
1	L + $CoSn_2$ + $\tau1$	L + $CoSn_2$ + $\tau1$
2	L + AuSn + $\tau1$	L + AuSn + $\tau1$
3	CoSn + $CoSn_2$ + $\tau1$	CoSn + $CoSn_2$ + $\tau1$
4	CoSn + AuSn + $\tau1$	CoSn + AuSn + $\tau1$
5	CoSn + $CoSn_2$ + $\tau1$	CoSn + $CoSn_2$ + $\tau1$
6	L + AuSn + αCo_3Sn_2	L + AuSn + αCo_3Sn_2
7	L + ζ + αCo_3Sn_2	L + ζ + αCo_3Sn_2
8	αCo + ζ + αCo_3Sn_2	αCo + ζ + αCo_3Sn_2
9	Au + αCo + β	Au + αCo + β

ternary interaction parameters of liquid, fcc, and hcp are assumed to be zero and only parameters of the ternary phase $\tau1$ and several binary IMCs are assessed to fit the phase relations and ternary homogeneities.

Combining the improved Au-Sn and Co-Sn system with the reassessed Au-Co binary system, the Au-Co-Sn ternary system was extrapolated to fit the available experimentally determined equilibria. The isothermal section of this ternary system at 653 K was calculated and is illustrated in Fig. 10, where the measured phase relations are also given, along with the three-phase regions additionally listed in Table IV. It is clear that all the phase relations are well assessed except for a slight deviation between

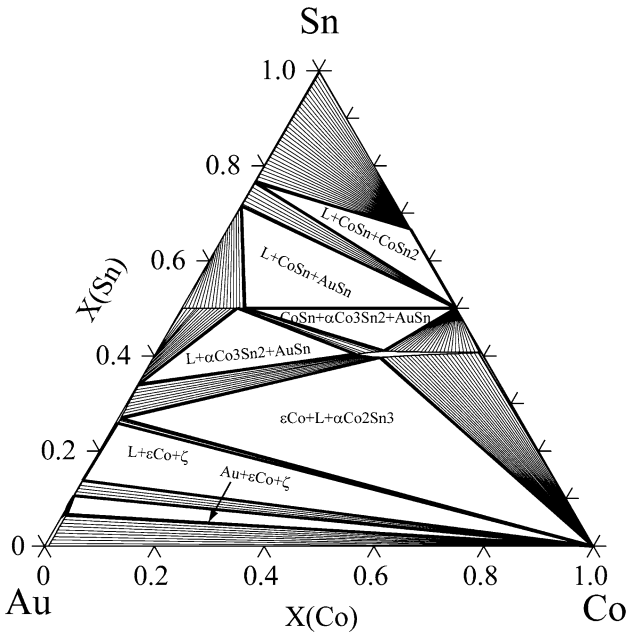

Fig. 11. Calculated isothermal section of the Au-Co-Sn ternary system at 669 K.

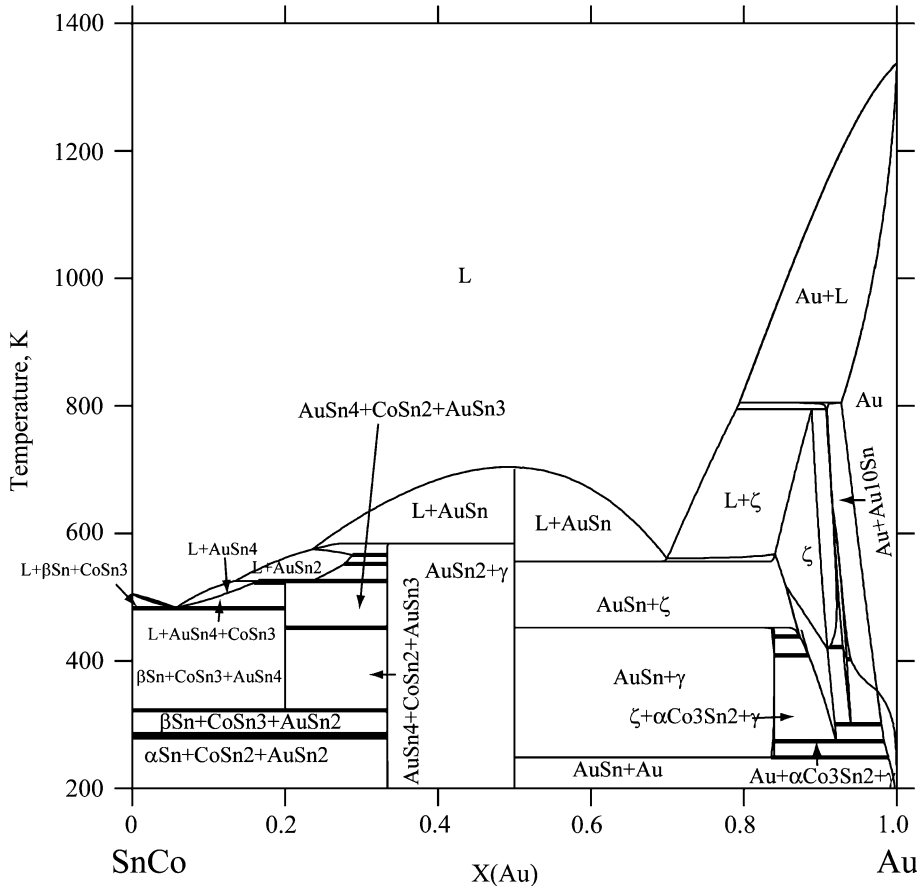

Fig. 12. Calculated Au-SnCo vertical section across the E2 eutectic point of the Au-Co-Sn ternary system.

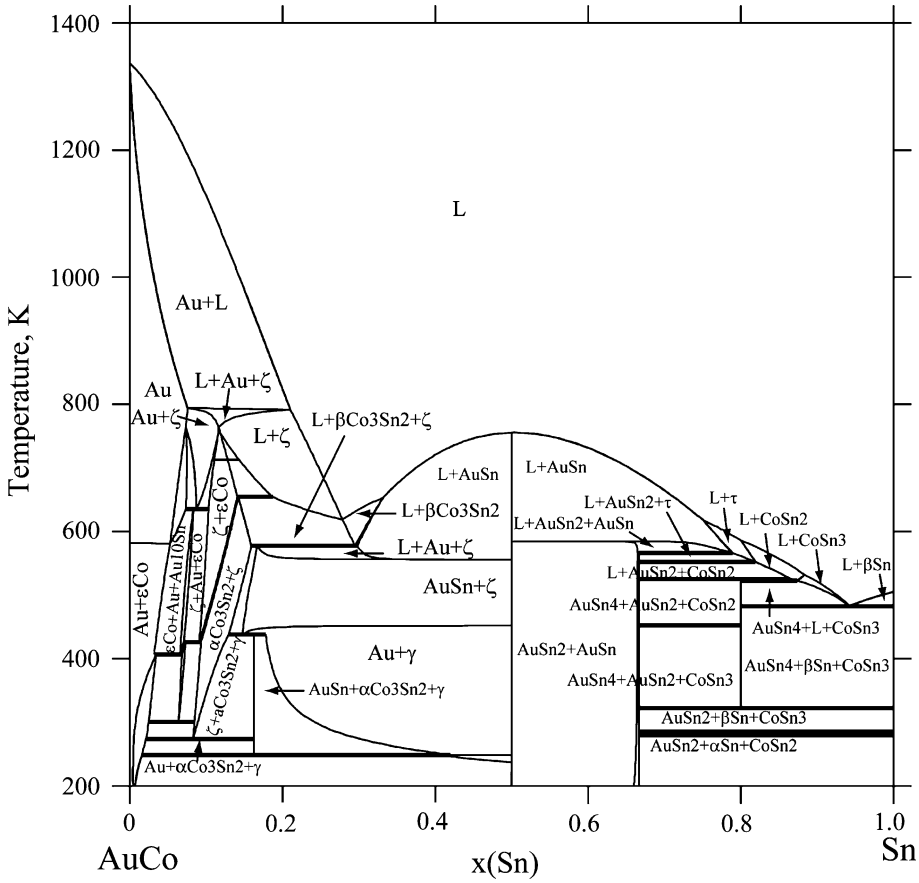

Fig. 13. Calculated AuCo-Sn vertical section across the E2 eutectic point of the Au-Co-Sn ternary system.

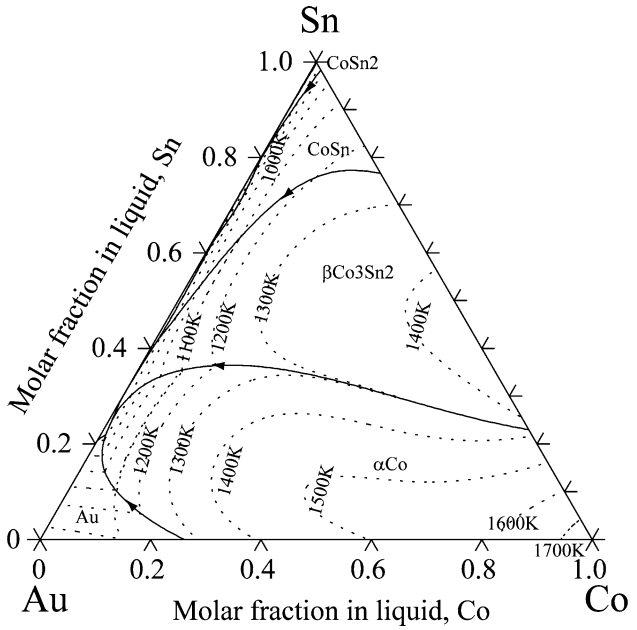

Fig. 14. Extrapolated liquidus projection of the Au-Co-Sn ternary system; dashed lines represent isothermal lines.

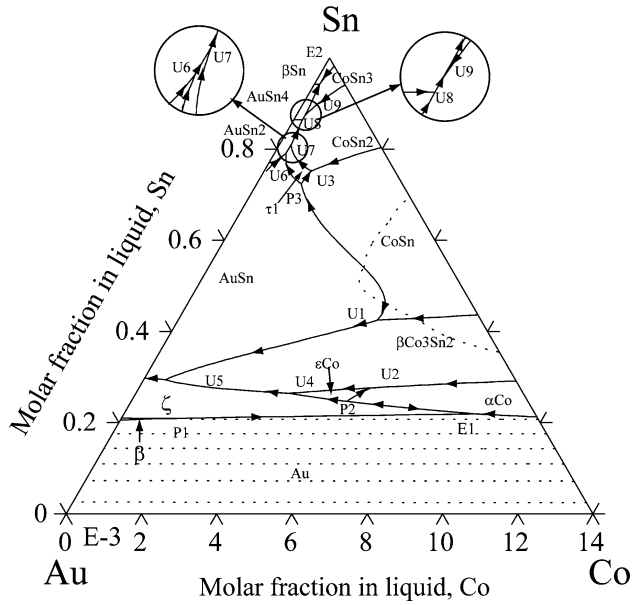

Fig. 15. Calculated liquidus projection of the Au-Sn-rich side of the Au-Co-Sn system.

the calculated and measured homogeneities for AuSn and αCo_3Sn_2, for which AuSn is calculated to contain 11.4 at.% Co and αCo_3Sn_2 24.5 at.% Au, in comparison with the experimental data of 12 at.% Co and 23 at.% Au, respectively.

Furthermore, the isothermal section at 669 K was calculated (Fig. 11). It could be found that the $\tau 1$

Table V. Calculated Invariant Reactions in the Au-Co-Sn Ternary System

Type	Reaction	T (K)
U_1	$L + CoSn \Leftrightarrow \beta Co_3Sn_2 + AuSn$	781.4
U_2	$L + \alpha Co \Leftrightarrow \beta Co_3Sn_2 + \varepsilon Co$	696.7
U_3	$L + CoSn \Leftrightarrow CoSn_2 + \tau 1$	660.6
U_4	$L + \varepsilon Co \Leftrightarrow \zeta + \beta Co_3Sn_2$	654.2
U_5	$L + \beta Co_3Sn_2 \Leftrightarrow AuSn + \zeta$	577.0
U_6	$L + AuSn \Leftrightarrow \tau 1 + AuSn_2$	565.8
U_7	$L + \tau 1 \Leftrightarrow AuSn_2 + CoSn_2$	552.2
U_8	$L + AuSn_2 \Leftrightarrow CoSn_2 + AuSn_4$	525.5
U_9	$L + CoSn_2 \Leftrightarrow CoSn_3 + AuSn_4$	522.5
E_1	$L \Leftrightarrow Au + \alpha Co + \zeta$	761.5
E_2	$L \Leftrightarrow CoSn_3 + AuSn_4 + \beta Sn$	483.0
P_1	$L + Au + \beta \Leftrightarrow \zeta$	795.1
P_2	$L + \alpha Co + \zeta \Leftrightarrow \varepsilon Co$	697.1
P_3	$L + AuSn + CoSn \Leftrightarrow \tau 1$	667.9

phase is absent at this temperature, which is in accordance with experimental results.[18] The vertical sections across the eutectic point of E2 (SnCo-Au and AuSn-Co) and liquidus projection were further calculated and are shown in Figs. 12–15. In addition, the invariant reactions in this system are listed in Table V. Figures 12 and 13 indicate that a new kind of solder with lower melting temperature than that of Au-30 at.% Sn solder, i.e., 553 K, can be designed based on the eutectic point of E2. With the help of this information, the sequence of solder–substrate interactions may also be predicted, i.e., which IMC may form.[51,52]

CONCLUSIONS

With the help of *ab initio* calculation, phase relations in the Au-Co-Sn ternary system have been thermodynamically assessed by the CALPHAD method. A set of thermodynamic parameters describing various phases in this system has been obtained that can reliably reproduce most of the experimental information. Some useful sections including isothermal and vertical sections have been further extrapolated, which may be useful for designing solder alloys.

ACKNOWLEDGEMENTS

This work was financially supported by the National Natural Science Foundation of China (Grant No. 50671122). Special acknowledgements are given for the Thermo-Calc software from Thermo-Calc AB, Stockholm Technology Park, Sweden, and the Pandat program, licensed from CompuThermo, LLC, Madison, WI, USA.

REFERENCES

1. R.J. Klein Wassink, *Soldering in Electronics*, 2nd ed. (Port Erin, Isle of Man: Electrochemical Publications, 1989).
2. K.N. Tu and K. Zeng, *Mater. Sci. Eng. R.* 34, 1 (2001).
3. R.J. Fields, S.R. Low III, and G.K. Lucey, *Metal Science of Joining*, ed. M.J. Cieslak, J.H. Perepezko, S. Kang, and M.E. Glicksman (Warrendale, PA: TMS, 1992), p. 165.
4. S.F. Dirnfeld and J.J. Ramon, *Weld. J.* 69, 373 (1990).
5. C.Y. Liu, C. Chen, A.K. Mal, and K.N. Tu, *J. Appl. Phys.* 85, 3882 (1999).
6. J. Kim, D. Kim, and C.C. Lee, *IEEE Trans. Adv. Packag.* 29, 473 (2006).
7. J. Kim and C.C. Lee, *Mater. Sci. Eng. A* 417, 143 (2006).
8. J.H. Kuang, M.T. Sheen, C.H. Chang, C.C. Chen, G.L. Wang, and W.H. Cheng, *IEEE Trans. Adv. Packag.* 24, 563 (2001).
9. G. Elger, M. Hutter, H. Oppermann, R. Aschenbrenner, H. Reichl, and E. Jäger, *Microsyst. Technol.* 7, 239 (2002).
10. J.W.R. Tew, X.Q. Shi, and S. Yuan, *Mater. Lett.* 58, 2695 (2004).
11. T. Yamamoto, S. Sakatani, S. Kobayashi, K.F. Keisuke, M. Ishio, and K. Shiomi, *Mater. Trans. JIM* 46, 2406 (2005).
12. W.J. Zhu, H.S. Liu, J. Wang, and Z.P. Jin, *J. Alloys Compd.* 456, 113 (2008).
13. F. Gao, T. Takemoto, and H. Nishikawa, *Mater. Sci. Eng. A* 420, 39 (2006).
14. L. Liu, C. Anderson, and J. Liu, *J. Electron. Mater.* 33, 935 (2004).
15. C.P. Vassilev, K.I. Lilova, and J.C. Gachon, *Intermetallics* 15, 1156 (2007).
16. T. Laurila, V. Vuorinen, and J.K. Kivilahti, *Mater. Sci. Eng. R* 49, 1 (2005).
17. C.W. Huang and K.L. Lin, *J. Electron. Mater.* 35, 2135 (2006).
18. A. Neumann, A. Kjekshus, C. Rømming, and E. Røst, *J. Alloys Compd.* 240, 42 (1996).
19. K.C. Hari Kumar, P. Wollants, and L. Dalaey, *CALPHAD* 18, 71 (1994).
20. G. Kresse and J. Furthmuller, *Phys. Rev. B* 54, 11169 (1996).
21. G. Kresse and J. Furthmuller, *Comput. Mater. Sci.* 6, 15 (1996).
22. M. Jiang, J. Sato, I. Ohnuma, R. Kainuma, and K. Ishida, *CALPHAD* 28, 213 (2004).
23. H.S. Liu, C.L. Liu, K. Ishida, and Z.P. Jin, *J. Electron. Mater.* 3, 1290 (2003).
24. J.O. Anderson, T. Helander, L. Hoglund, P. Shi, and B. Sundman, *CALPHAD* 26, 273 (2002).
25. PANDAT software for multicomponent phase diagram calculations by CompuTherm. (LLC, Madison, WI, since 2000).
26. V. Grolier and R. Schmid-Fetzer, *Int. J. Mater. Res.* 98, 797 (2007).
27. H. Okamoto, T.B. Massalski, M. Hasebe, and T. Nishizawa, *Bull. Alloy Phase Diagrams* 6, 449 (1985).
28. J. Korb, unpublished assessment, GTT-Technologies, (2004).
29. A.T. Dinsdale, *CALPHAD* 15, 317 (1991).
30. W. Wahl, *Z. Anorg. Chem.* 66, 60 (1910).
31. U. Hashimoto, *J. Jpn. Inst. Met.* 1, 177 (1937).
32. E. Raub and P. Walter, *Z. Metallkd.* 41, 234 (1950).
33. A.T. Grigor'ev, E.M. Sokolovskaya, and M.V. Maksimova, *Zh. Neorg. Khim.* 1, 1047 (1956).
34. L. Weil, *Z. Phys. Chem.* 16, 368 (1958).
35. P. Taskinen, *Scand. J. Met.* 13, 39 (1984).
36. W. Klement Jr., *Trans. Met. Soc. AIME* 227, 965 (1963).
37. V.V. Berezutskiy, V.N. Eremenko, and G.M. Lukashenko, *Izvest. Akad.Nank SSSR Metally* 54 (1975).
38. A. Kubil and C.B. Alcol, *Met. Sci. J.* 1, 19 (1967).
39. S.S. Wang and J.M. Toguri, *Can. J. Chem.* 51, 2362 (1973).
40. B. Predel and E. Zehnpfund, *Z. Metallkd.* 64, 782 (1973).
41. L. Topor and O.J. Kleppa, *Metall. Trans. B* 15, 573 (1984).
42. P.E. Blöchl, *Phys. Rev. B* 50, 17953 (1994).
43. G. Kresse and J. Joubert, *Phys. Rev. B* 59, 1758 (1999).
44. J.P. Perdew and Y. Wang, *Phys. Rev. B* 45, 13244 (1992).
45. J.P. Perdew, J.A. Chevary, S.H. Vosko, K.A. Jackson, M.R. Pederson, and D.J. Singh. *Phys. Rev. B* 46, 6671 (1992).
46. H.J. Monkhorst and J.D. Pack, *Phys. Rev. B* 13, 5188 (1976).

47. M. Methfessel and A.T. Paxton, *Phys. Rev. B* 40, 3616 (1989).
48. S. Lidin and A.K. Larsson, *J. Solid State Chem.* 118, 313 (1995).
49. A.K. Jena and M.B. Bever, *Metall. Trans. B* 10, 545 (1979).
50. H. Okamoto, *J. Phase Equilib.* 14, 765 (1993).
51. K. Zeng and J.K. Kivilahti, *J. Electron. Mater.* 30, 35 (2001).
52. C.L. Liu, Z.P. Jin, and H.S. Liu, *Chin. J. Nonferr. Met.* 13, 1343 (2003).